Arabian Journal of Chemistry (2019) **12**, 1652–1659

King Saud University

Arabian Journal of Chemistry

www.ksu.edu.sa
www.sciencedirect.com

ORIGINAL ARTICLE

Electrical conductivity and ion-exchange kinetic studies of polythiophene Sn(VI)phosphate nano composite cation-exchanger

Anish Khan *, Abdullah M. Asiri, Aftab Aslam Parwaz Khan, Sher Bahadar Khan

Chemistry Department, King Abdulaziz University, Jeddah 21589, Saudi Arabia
Center of Excellence for Advanced Materials Research, King Abdulaziz University, P.O. Box 80203, Jeddah 21589, Saudi Arabia

Received 22 May 2013; accepted 2 September 2014
Available online 23 September 2014

KEYWORDS

Nanotetrapod;
Hybrid;
Electrically conducting;
Diffusion coefficient;
Ion-exchange;
Kinetics

Abstract A polymeric hybrid nanocomposite, namely polythiophene tin(IV)phosphate (PTh–SnP), was expediently synthesized by incorporating polythiophene (PTh) in tin phosphate (SnP) to enhance the conducting behavior and sorption of heavy metal ions by porous polymeric cation exchanger. Composite was characterized by Fourier Transform-Infra Red and Transmission Electron Microscopy. The dc electrical conductivity studies carried out on the composite, showed conductivity within the range of 4.0×10^{-2}–1.0×10^{-3} S/cm^{-1}; measured by a 4-in line-probe dc electrical conductivity measuring technique. Ion-exchange kinetics for few divalent metal ions was evaluated by particle diffusion-controlled ion-exchange phenomenon at four different temperatures. The particle diffusion mechanism is confirmed by the linear τ (dimensionless time parameter) vs t (time) plots. The exchange processes thus controlled by the diffusion within the exchanger particle for the systems studies herein. Some physical parameters like self-diffusion coefficient (D_0), energy of activation (E_a) and entropy ($\Delta S°$) have been evaluated under conditions favoring a particle diffusion-controlled mechanism.

1. Introduction

Nano-size composites have attracted a great deal of interests because of their unique structural, electrical and mechanical properties. Their potential applications in various fields include material chemistry (Bahr and Tour, 2005), nanoscale devices (Ebbesen, 1996; Treay et al., 1996) and field emission (Deheer et al., 1995). Various approaches have been developed to stimulate the hybridization of materials to form a nano composite that might be used as catalyst in separation and storage technology (Ruoff et al., 1993; Tomita et al., 1993;

* Corresponding author at: Chemistry Department, King Abdulaziz University, Jeddah 21589, Saudi Arabia. Mobile: +966 559631440.
E-mail address: anishkhan97@gmail.com (A. Khan).
Peer review under responsibility of King Saud University.

Production and hosting by Elsevier

http://dx.doi.org/10.1016/j.arabjc.2014.09.004

Seraphin et al., 1993; Saito et al., 1993) there also are potentially new and attractive applications for modern or novel devices/processes which require the development of materials with new thermal, magnetic and electrical properties (Wang et al., 2004). Electrically conducting conjugated polymers such as polyparaphenylene, polythiophene (PTh), polyaniline, polypyrrole and polyacetylene have received considerable attention of researchers because of their curious electronic, magnetic and optical properties (Shirakawa, 2002; MacDiarmid, 2002; Heeger, 2002).

In recent years polymeric-inorganic composites have attracted great interest, both in industry and academics, because they often exhibit remarkable improvement in material properties when compared with conventional polymers. These improvements can include high elastic moduli (Okada et al., 1990; Giannelis, 1996; Giannelis et al., 1999; LeBaron et al., 1999; Vaia et al., 1999; Biswas and Ray, 2001), increased strength and heat resistance (Giannelis, 1998), decreased gas permeability (Xu et al., 2001; Bharadwaj, 2001; Messersmith and Giannelis, 1995; Kojima et al., 1993) and flammability (Gilman et al., 1997, 2000; Gilman, 1999; Dabrowski et al., 1999; Bourbigot et al., 2000). Polymeric-inorganic composite materials prepared by incorporation of organic polymer into the inorganic material are a new class of composites used in ion-exchange chromatography. Their chemical, thermal and mechanical stabilities promote the reproducibility of results obtained from chromatographic studies. A number of such materials were prepared in the laboratory by incorporating, polyaniline, polypyrrole, polyanisidine and poly-*o*-toluidine into the precipitate of an element belonging to column III, IV, V and VI of the periodic table (Clearfield, 2000; Niwas et al., 1998, 1999; Khan and Alam, 2003; Varshney et al., 1998, 2001; Zhang et al., 1996; Alberti et al., 1995). Electrical conductivity (in the semiconducting region) with the chromatographic behavior of these composites attracted researchers for more possible application in the field of environmental science engineering.

It was therefore, in our present work, considered to synthesize such hybrid ion-exchangers with a good ion-exchange capacity, high stability, reproducibility and selectivity for heavy metal ions, possessing its useful techno application.

To the best of our knowledge PTh–SnP composite formed by *in situ* chemical oxidative polymerization method has not been studied yet. Therefore we explored the usage of properties of the PTh–SnP conducting composite for the synthesis of new types of nanocomposite materials.

2. Experimental procedure

2.1. Reagents and instruments

The main reagents (thiophene monomer; E. Merck, stannic chloride from CDH and orthophosphoric acid by Loba Chemie) were used. All other reagents (hydrochloric acid, nitric acid, sulfuric acid, sodium nitrate, potassium nitrate, mercuric nitrate, lead nitrate etc.) and chemicals were of analytical grade. The following instruments were used during present research work: an electronic balance (digital, Sartorius-21OS, Japan), and an automatic temperature controlled water bath incubator shaker - Elcon (India). Aqueous solutions of different concentrations were prepared by dilution of standard salt solutions in deionized water (18.6 M Ω cm^{-1}) from Milli-Q plus of Millipore, USA. FTIR spectrophotometer model 2000 (Perkin Elmer, USA) was used for functional group analysis.

2.2. Preparation of polythiophene Sn(IV) phosphate (PTh–SnP)

The PTh–SnP cation-exchanger was prepared by the sol–gel mixing of polythiophene, an organic polymer, into the inorganic precipitate of Sn(IV) phosphate prepared as described by Khan et al. Khan and Khan (2007). The synthesis of PTh–SnP composite was as follows: 100 mL of $CHCl_3$ solution containing SnP (0.5 g) was added to a 500-mL, double-necked, round-bottom flask equipped with a magnetic, Teflon-coated stirrer. The mixture was sonicated for 50 min at room temperature to disperse the SnP. $FeCl_3$ (2 g) in 100 mL of $CHCl_3$ solution was added to the solution, which was further sonicated for 50 min at room temperature. The thiophene monomer (0.5 mL) with 50 mL of $CHCl_3$ solution was placed in the small portion line of the double necked flask and added gradually (dropwise and slowly) into the suspension solution with constant stirring. The reaction mixture was stirred for an additional 24 h under the same conditions. The resultant PTh–SnP powder was precipitated in methanol, filtered with a Buchner funnel, and then carefully washed with methanol, hydrochloric acid (0.1 M), distilled water and acetone. The obtained whitish black powder was dried under a vacuum dryer at room temperature for 24 h. PTh was synthesized with a similar method, and the same molar ratios of monomer to dopant were incorporated into the polymerization.

The samples were converted to the H^+ form by keeping it in 1 M HNO_3 solution for 24 h with occasional shaking, and intermittent replacement of the supernatant liquid. The excess acid was removed by washing several times with DMW (dematerialized water). The samples were finally dried at 40 °C. Hence a number of PTh–SnP samples were prepared and on the basis of Na^+ ion exchange capacity (IEC) (2.8 meq/g) and physical appearance was selected for further studies.

2.3. Transmission electron microscopy (TEM)

Fine particle dispersion method was used for sample preparation in which sample material PT-1 was ground using mortar and pestle to obtain fine particles. The fine particles were dispersed in a volatile liquid (alcohol) by stirring which separated the agglomerated particles and ensured a homogenous suspension. The dilution step is often required in order to obtain very low concentrations of the material, so that the particles on the support film remain isolated. A droplet of the sample suspension is then placed on the copper coated grid. The specimen is ready for observation after complete evaporation or drying. TEM was performed on a CM 200 Phillips microscope with an acceleration voltage of 200 kV to determine the particle size of the PTh–SnP composite cation-exchange material.

2.4. Electrical conductivity measurements

The composite sample was treated with 1 M aqueous solution of HCl and washed with DMW to remove excess HCl. The sample material was dried completely between 40 and 50 °C in an oven. Then 200 mg material was finely ground in a

mortar and pestle and pellets were made at room temperature with the help of a hydraulic pressure instrument at 25 KN pressure for 20 min. The thickness of pellet was measured by a micrometer. Four-probe electrical conductivity measurements with increasing temperatures (between 35 and 200 °C) for the composite samples were performed on pressed pellets by using a 4-in-line-probe dc electrical conductivity-measuring technique.

2.5. Kinetic measurements

The composite cation-exchange material was treated with 1 M HNO_3 for 24 h at room temperature with occasional shaking. Intermittently the supernatant liquid was replaced with fresh acid to ensure complete conversion to the H^+-form and the excess acid was removed after several washings with DMW. Then the dried ion-exchanger sample in the H^+-form was ground and then sieved to obtain particles of definite mesh sizes. From these, the particles of mean radius ~125 μm (50–70 mesh) were used to evaluate various kinetic parameters. The rate of exchange was determined by the limited bath technique as follows. Twenty milliliter fractions of the 0.03 M metal ion solutions (Mg, Ca, Sr, Ba, Ni, Cu, Mn and Zn) were shaken with 200 mg of the cation-exchanger in H^+-form in several stoppered conical flasks at the desired temperatures [20, 30, 40 and 50 °C] for different time intervals (0.5, 1.0, 2.0, 3.0 4.0 and 5.0 min). The supernatant liquid was removed immediately and determinations were made, usually by EDTA titration. Each set was repeated four times and the mean value was taken for calculations.

3. Results and discussions

Tetrapod nano organic–inorganic composite cation-exchange material was prepared in this study by incorporation of the electrically conducting polymer, polythiophene, into inorganic matrices of fibrous Sn(IV) phosphate. Composite for the further ion-exchange studies, since it is a new nanostructure with higher surface-to-volume ratio that could give better ion-exchange kinetics, reproducible behavior and chemical and thermal stability.

3.1. Characterization

It is clear from the TEM studies that the morphology of the material was found nano as indicated in Fig. 1a. From the deep morphological determination of the composite, it is clear from the TEM (Fig. 1b and c) that morphologically the composite is a nano tetra pod like structure and not homogeneously distributed.

The FTIR spectra of the PTh, SnP and PTh–SnP composites are shown in Fig. 2. Within the spectrum of PTh (Fig. 2(a)), there are several low-intensity peaks in the range of 2800–3100 cm^{-1} that can be attributed to the aromatic C—H stretching vibrations and C=C characteristic band (1637 cm^{-1}) Wang and Rubner, 1990; Wang, 1996. The absorption in this region is obscured by the bipolaron absorption of the doped PTh. The range of 600–1500 cm^{-1} is the fingerprint region of PTh. The peak at 786 cm^{-1} is usually ascribed to the C—H out-of-plane deformation mode, whereas other peaks in this region are attributed to the ring stretching, and C—H in-plane deformation modes (Roncoli, 1992; Toshima and Hara, 1995). The C—S bending mode has been identified at approximately 690 cm^{-1} and indicates the presence of a thiophene monomer (Udum et al., 2005).

The PTh–SnP composites (Fig. 2(b)) show nearly identical numbers and positions of the IR bands in the range of 600–3200 cm^{-1}. The C—H stretching vibrations and C=C characteristic peaks can be identified almost in the same range at 2800–3100 and 1637 cm^{-1}, respectively. Only the ring-deformation modes are shifted because of polaron-polaron interaction between the planar PTh backbone and SnP, indicating that some of them (SnP) do not fully interact with the PTh molecules because of the bulky group.

3.2. Electrical conducting behavior of PTh–SnP nano-composite

Electrical conductivities of the pellets of PTh–SnP composite samples were determined from the measurement of conductivity of the samples using the four-probe method (Instruction Manual, 2000) of conductivity measurement for semiconductors. This is the most satisfactory method as it overcomes difficulties which are encountered in conventional methods of conductivity measurement (i.e., two probe), e.g., the rectifying nature of the metal-semiconductor contacts and the injection of minority carriers by one of the current-carrying contacts, which affects the potential of the other contacts and modulates the conductance of the material, etc. The current–voltage data generated at increasing temperatures for the determination of electrical conductivity of the composite sample were processed for the calculation of electrical conductivity using the following equation:

$$\rho = \rho_0 / G_7(W/S) \tag{1}$$

where ρ is corrected resistivity (Ω cm), ρ_0 = uncorrected resistivity (Ω cm), $G_7(W/S)$ is the correction factor used in the case of a no conducting bottom surface, which is a function of W, the thickness of the sample under test (cm) and S, the probe spacing (cm); i.e.

$$G_7(W/S) = (2S/W)\ln 2 \tag{2}$$

$$\rho_0 = V/I \times 2\pi S, \tag{3}$$

$$\sigma = \frac{1}{\rho} \tag{4}$$

where I is the current (A), V is the voltage (V) and σ = dc electrical conductivity (s/cm). Although the electrical conductivity measurements were done under ambient conditions, the composite samples were thoroughly dried before making the pellets and performing the electrical conductivity measurements. Hence, the contribution of protonic conductivity to the total electrical conductivity due to the presence of moisture should be minimum and need not be taken into consideration.

The main constituent that makes the composite electrically conductive is PTh. The conducting properties depend on the percolation behavior of the conducting phase. The electrical conductivity of the composite is due to oxidized PTH maintained in its conductive state by PTh–SnP counter ions in excess. The variation of electrical conductivity (σ) of the composite samples with increasing temperatures (between 35 and 200 °C) was investigated. On examination, it was observed that the electrical conductivities of the samples increase with an

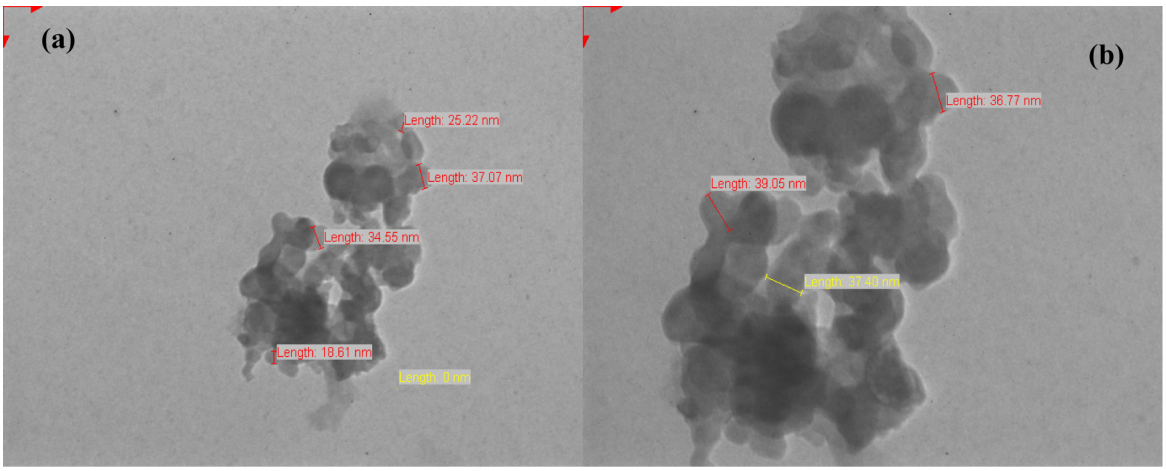

Figure 1 TEM images of nano tetrapod composite (a) and (b) at different magnification.

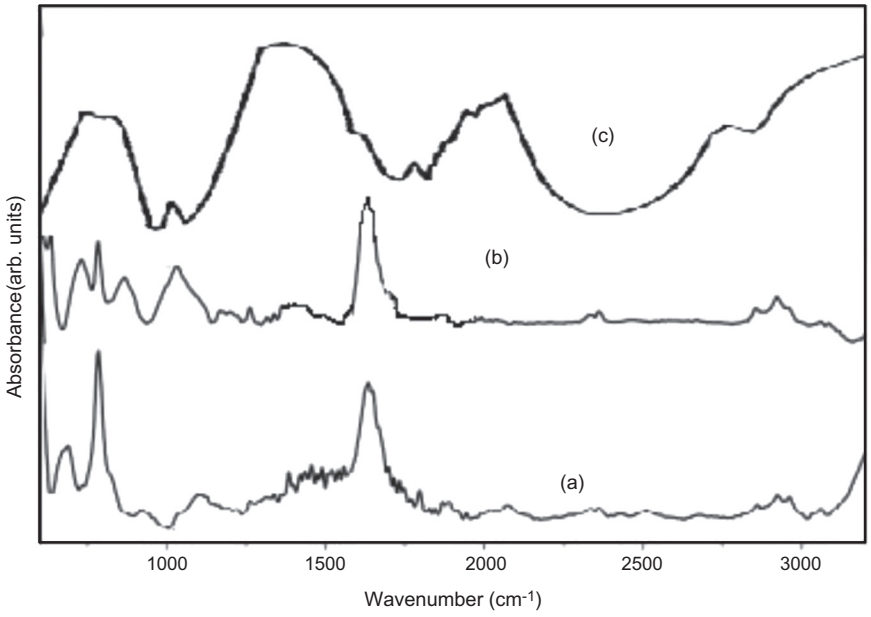

Figure 2 FTIR spectrum of (a) polythiophene; (b) composite and (c) tin phosphate.

increase in temperature and the values are of the order 1.0×10^{-3}–4.0×10^{-2} S cm^{-1}, i.e., in the borderline of the conductor and semiconductor region. To determine the nature of the dependence of electrical conductivity on temperature, plots of $\log \sigma$ versus $1000/T$ (K) were drawn (Fig. 3) and they followed the Arrhenius equation similarly to other semiconductors (Mohammad, 2000).

The thermal stability of the composite material (HCl treated) in terms of dc electrical conductivity retention was studied under isothermal conditions (at 50, 80, 110 and 140 °C) using 4-probe-in-line dc electrical conductivity measurements at 30 °C intervals. The electrical conductivity measured with respect to the time of accelerated ageing. It was observed that the electrical conductivity is quite stable at 50, 80, 110 and 140 °C, which supports the fact that the dc electrical conductivity of the composites is sufficiently stable under ambient temperature conditions. The electrical conductivity decreases with time at 150 °C, which may be attributed to the loss of dopant and the chemical reaction of dopant with the material. The material was also observed to be a stable material, i.e., the room temperature conductivity is negligibly affected by short-term exposure to laboratory air.

The conductivity of PTh–SnP nano-composite synthesized presently is high may be due to the electron donating property of the SnP group. The conductivity of the composite by self doped polymerization (as prepared) increases by increasing temperature up to 130 °C. This increase in conductivity with increase in temperature is the characteristic of "Thermal activated behavior" (Zuo et al., 1987) The increase in conductivity could be due to the increase in the efficiency of charge transfer between the composite chains and the dopant with an increase in the temperature, (Bayashi et al., 1993) It is also possible that the thermal curing affects of the chain alignment of the polymeric inorganic composite, which leads to the increase in conjugation length and that brings about the increase in conductivity.

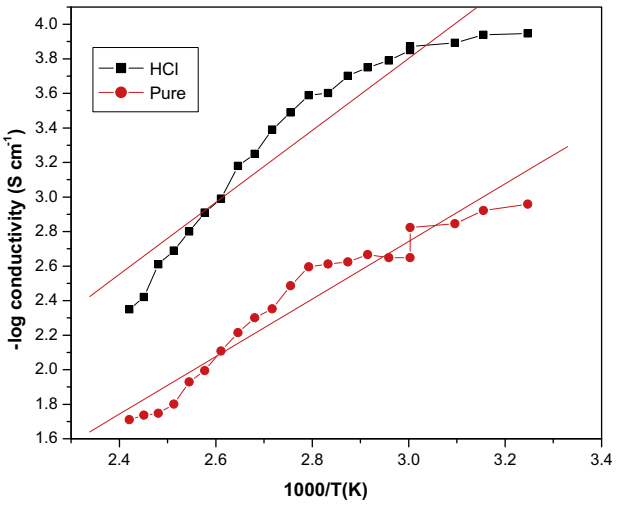

Figure 3 Arrhenius plots for four probe electrical conductivity of pure and HCl treated at different temperatures for nano-composite.

3.3. Ion-exchange kinetics of PTh–SnP nano tetrapod-composite

Kinetic measurements were made under conditions favoring a particle diffusion-controlled ion-exchange phenomenon for the exchange of Mg(II)–H(I), Ca(II)–H(I), Sr(II)–H(I), Ba(II)–H(I), Ni(II)–H(I), Cu(II)–H(I), Mn(II)–H(I) and Zn(II)–H(I). The particle diffusion controlled phenomenon is favored by a high metal ion concentration, a relatively large particle size of the exchanger and vigorous shaking of the exchanging mixture. The infinite time of exchange is the time necessary to obtain equilibrium in an ion exchange process. The ion exchange rate becomes independent of time after this interval. Fig. 4 shows that 30 min was required for the establishment of equilibrium at 40 °C for Cu^{2+}–H^+ exchange. Similar behavior was observed for Ca^{2+}–H^+, Sr^{2+}–H^+, Ba^{2+}–H^+, Ni^{2+}–H^+, Mg^{2+}–H^+, Mn^{2+}–H^+ and Zn^{2+}–H^+ exchanges. Therefore, 40 min was assumed to be the infinite time of exchange for the system. A study of the concentration effect on the rate of exchange at 30 °C showed that the initial rate of exchange was proportional to the metal ion concentration at and above 0.07 M (Fig. 5). Below the concentration of 0.07 M, film diffusion control was more prominent. The results are expressed in terms of the fractional attainment of equilibrium, $U(\tau)$ with time according to the equation

$$U(\tau) = \frac{\text{the amount of exchange at time '}t\text{'}}{\text{the amount of exchange at inf inite time}}. \quad (5)$$

On the basis of plots of $U(\tau)$ versus t (min) for all metal ions, indicated that the fractional attainment of equilibrium was faster at higher temperature suggesting that the mobility of the ions increased with an increase in temperature and the uptake decreased with time. Each value of $U(\tau)$ will have a corresponding value of τ, a dimensionless time parameter. On the basis of the Nernst–Planck equation, the numerical results can be expressed by explicit approximation (Helfferich and Plesset, 1958; Plesset et al., 1958).

$$U(\tau) = \left\{1 - \exp\left[\pi^2\left(f_1(\alpha)\,\dot{t} + f_2(\alpha)\,\tau^2 + f_3(\alpha)\,\tau^3\right)\right]\right\}^{1/2} \quad (6)$$

where τ is the half time of exchange $= \bar{D}_{H^+} t/r_o^2$, α is the mobility ratio $= \bar{D}_{H^+}/\bar{D}_{M^{2+}}$ r_0 is the particle radius, $\bar{D}_{H^+}$ and $\bar{D}_{M^{2+}}$ are the inter diffusion coefficients of counter ions H^+ and M^{2+}, respectively in the exchanger phase. The three functions $f_1(\alpha)$, $f_2(\alpha)$ and $f_3(\alpha)$, depend upon the mobility ratio (α) and the charge ratio ($Z_{H^+}/Z_{M^{2+}}$) of the exchanging ions. Thus they have different expressions as given below. When the exchanger is taken in the H^+ form and the exchanging ion is M^{2+}, for $1 \leqslant \alpha \leqslant 20$, as in the present case, the three functions have the values:

$$f_1(\alpha) = -\frac{1}{0.64 + 0.36\alpha^{0.668}}, \quad (7)$$

$$f_2(\alpha) = -\frac{1}{0.96 - 2.0\alpha^{0.4635}}, \quad (8)$$

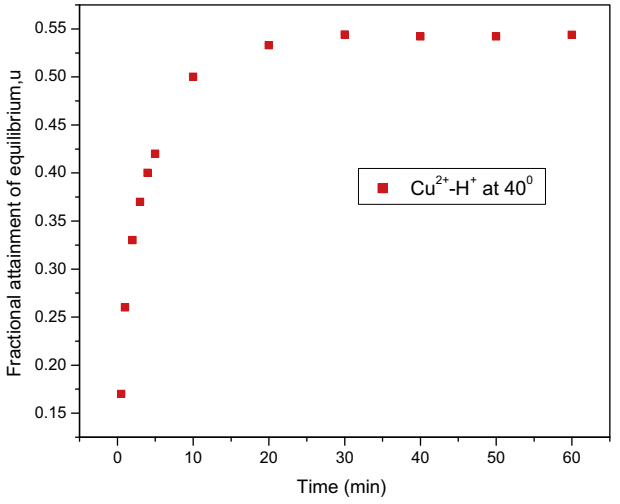

Figure 4 A plot of $U(\tau)$ vs. t for M(II)–H(I) exchanges at 40 °C on a nano-composite cation exchanger for the determination of infinite time.

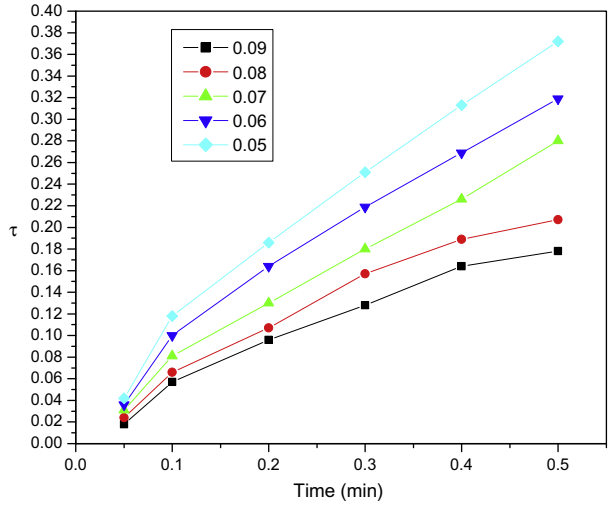

Figure 5 A plot of τ vs. t (time) for M(II)–H(I) exchanges at 30 °C on a nano-composite cation exchanger using different metal solution concentrations.

$$f_3(\alpha) = -\frac{1}{0.27 + 0.09\alpha^{1.140}}, \quad (9)$$

The value of τ is obtained on solving Eq. (6) using a computer. The plots of τ versus time (t) at four temperatures, showed straight lines passing through the origin, confirming the particle diffusion control phenomenon for M(II)–H(I) exchanges at a metal ion concentration of 0.07 M. The slopes (S values) of various τ versus time (t) plots are given in Table 1. The S values are related to $\bar{D}_{H^+}$ as follows:

$$S = \bar{D}_{H^+}/r_0^2, \quad (10)$$

The values of $-\log \bar{D}_{H^+}$ obtained by using Eq. (10) plotted against $1/T$ are straight lines as shown in Fig. 6, thus verifying the validity of the Arrhenius relation;

$$\log \bar{D}_{H^+} = D_0 \exp(-E_a/RT). \quad (11)$$

D_0 is obtained by extrapolating these lines and using the intercepts at the origin. The activation energy (E_a) is then calculated with the help of the Eq. (11), putting the value of $\bar{D}_{H^+}$ at 273 K. The entropy of activation ($\Delta S°$) was then calculated by substituting D_0 in Eq. (11)

$$D_0 = 2.72d^2(kT/h)\ \exp(\Delta S°/R) \quad (12)$$

where d is the ionic jump distance taken as 5 A^0 (Barrer et al., 1961), k is the Boltzmann constant, R is the gas constant, h is Plank's constant and T is taken as 273 K. The values of the diffusion coefficient (D_0), energy of activation (E_a) and entropy of activation ($\Delta S°$) thus obtained are summarized in Table 2. The kinetic study reveals that equilibrium is attained faster at higher temperature, probably because of a higher diffusion rate of ions through the thermally enlarged interstitial positions of the ion-exchange matrix. The particle diffusion phenomenon is evident from the straight lines passing through the origin for τ versus time (t) plots. Positive values of the entropy suggest a greater degree of order achieved during the forward ion-exchange in the M(II)–H(I) process. From Table 2, it is observed that the self-diffusion co-efficient is highest for the Ba^{2+} ion. As ionic radius of Ba^{2+} ion is greater, the

Table 1 Slopes of various τ versus time (t) plots on nano-composite cation exchanger at different temperatures.

Migrating ions	10^4 S (s^{-1})			
	20 °C	30 °C	40 °C	50 °C
Mg(II)	2.00	2.16	3.90	3.90
Ca(II)	1.10	2.11	1.88	2.00
Sr(II)	1.00	1.30	2.68	4.00
Ba(II)	1.40	2.00	2.42	3.05
Cu(II)	1.45	2.20	3.33	8.00
Ni(II)	2.15	2.50	3.07	4.30
Zn(II)	4.80	6.20	7.20	9.90
Mn(II)	2.15	3.33	5.20	7.70

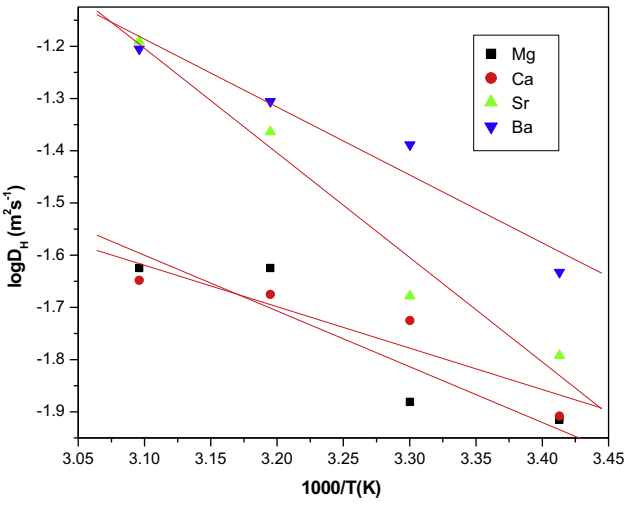

(A)

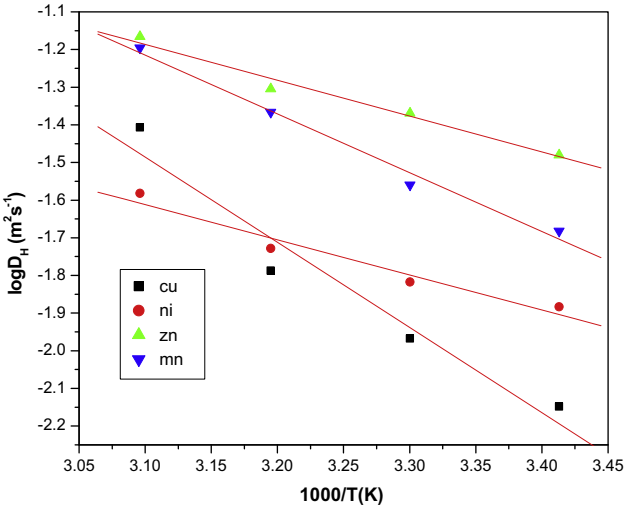

(B)

Figure 6 Plots of $-\log D_H^+$ vs. $1000/T$ (K) for (A) Mg(II), Ca(II), Sr(II), Ba(II) and (B) Cu(II), Ni(II), Zn(II) and Mn(II) on nano-composite cation exchanger.

Table 2 Values of D_0, E_a and $\Delta S°$ for the exchange of H(I) with some metal ions on nano-composite cation exchanger.

Metal ion exchange with H(I)	Ionic mobility ($m^2\ V^{-1}\ s^{-1}$)	Ionic radii (nm)	10^{10} D_0 ($m^2\ s^{-1}$)	E_a (k J mol^{-1})	$\Delta S°$ (J K^{-1} mol^{-1})
Mg(II)	55×10^{-9}	7.8×10^{-2}	1.7093	6.5477	0.1236
Ca(II)	62×10^{-9}	10.6×10^{-2}	0.8406	12.2939	0.0645
Sr(II)	62×10^{-9}	12.7×10^{-2}	5.001	41.4444	0.2124
Ba(II)	66×10^{-9}	14.3×10^{-2}	0.9719	7.8737	0.1655
Cu(II)	57×10^{-9}	7.0×10^{-2}	5.5285	37.4828	0.2207
Ni(II)	52×10^{-9}	7.8×10^{-2}	1.2817	161.8435	0.0992
Zn(II)	56×10^{-9}	8.3×10^{-2}	1.7647	117.4737	0.1258
Mn(II)	55×10^{-9}	9.1×10^{-2}	3.6252	57.1651	0.1856

Ba^{2+} ion is least hydrated and therefore its self-diffusion co-efficient is higher.

According to the value of self-diffusion co-efficient, the selectivity order of metal ions is $Cu^{2+} > Sr^{2+} > Mn^{2+} > Zn^{2+} > Mg^{2+} > Ni^{2+} > Ba^{2+} > Ca^{2}$. Further, it is observed that Ea values of metal ions in the order $Ni^{2+} < Zn^{2+} < Mn^{2+} < Sr^{2+} < Cu^{2+} < Ca^{2+} < Ba^{2+} < Mg^{2+}$ indicate the order of exchange process of metal ion. Lower the activation energy (E_a) stronger the preference for metal ion by the exchanger site. Similarly smaller the standard entropy change ($\Delta S°$) values indicate the preference of more active exchangeable site in the exchanger and strong preference for that metal ion (Varshney et al., 1997).

4. Conclusions

We synthesized tetrapod nano composites *in situ* chemical oxidative polymerization method of the thiophene monomer onto SnP. The characterization of the morphological structure indicated that the thiophene molecules are adsorbed and then polymerized on the surface of SnP, which has been used as the core in the formation of hybrid PTh–SnP composites. Finally, the improvements made in various physical properties of this composite are expected to enhance the application potential of conducting PTh without hampering its chemical properties. The method described here may be useful in developing new applications for PTh–SnP composites in molecular electronics and other fields. It behaves as an electrically conducting composite cation-exchanger. The electrical borderline semi-conducting behavior of this organic–inorganic composite material can be employed as a semiconductor in electrical and electronic devices. The feasibility of ion-exchange kinetics reveal that the mechanism of exchange to be particle diffusion as confirmed by the linear τ (dimensionless time parameter) vs t (time) plots. Further, various kinetic parameters like self-diffusion coefficient (D_0), energy of activation (E_a) and entropies ($\Delta S°$) have been evaluated under condition favoring a particle diffusion-controlled mechanism. The above studies thus reveal the promising use of PTh–SnP as a cation exchanger. The chemical, thermal and mechanical strength of this electroactive material can be utilized to make important for the environmentalists.

Acknowledgements

We are thankful to the Centre of Excellence for Advanced Materials Research (CEAMR), King Abdulaziz University, Saudi Arabia to carry out experiments on this work.

References

Alberti, G., Casciola, M., Dionigi, C., Vivani, R., 1995. In: Proceedings of International Conference on Ion-Exchange, ICIE '95, Takamtsu, Japan, December 1995, pp. 4–6.

Bahr, J.L., Tour, J.M., 2005. Covalent chemistry of single-wall carbon nanotubes. J. Mater. Chem. 12, 1952–1958.

Barrer, R.M., Bertholomew, R.F., Rees, L.V.C., 1961. The diffusion and sorption of water in zeolites intrinsic and self-diffusion. Phys. Chem. Solids 21, 12–24.

Bayashi, A.K.O., Ishikawa, H., Amano, K., Saton, M., Hasegawa, E., 1993. Electrical-conductivity of annealed polyaniline. J. Appl. Phys. 74 (I), 296–299.

Bharadwaj, R.K., 2001. Modeling the barrier properties of polymer-layered silicate nanocomposites. Macromolecules 34, 9189–9192.

Biswas, M., Ray, S., 2001. Recent progress in synthesis and evaluation of polymer-montmorillonite nanocomposites. Adv. Polym. Sci. 115, 167–221.

Bourbigot, S., LeBras, M., Dabrowski, F., Gilman, J.W., Kashiwagi, T., 2000. PA-6 clay nanocomposite hybrid as char forming agent in intumescent formulations. Fire Mater. 24, 201–208.

Clearfield, A., 2000. Inorganic ion exchangers, past, present, and future. Solvent Extr. Ion Exch. 18, 655–678.

Dabrowski, F., Bras, M.L., Bourbigot, S., Gilman, J.W., Kashiwagi, T., 1999. PA-6 montmorillonite nanocomposite in intumescent fire retarded EVA. In: Proceedings of the Eurofillers' 99, Lyon-Villeurbanne, France, September 1999, pp. 6–9.

Deheer, W.A., Chatelain, A., Ugarte, D.A., 1995. Science 270, 1179–1180.

Ebbesen, T.W., 1996. Carbon nanotubes. Phys. Today 49, 26–32.

Giannelis, E.P., 1996. Polymer layered silicate nanocomposites. Adv. Mater. 8, 29–35.

Giannelis, E.P., 1998. Polymer-layered silicate nanocomposites: synthesis, properties and applications. Appl. Organomet. Chem. 12, 675–680.

Giannelis, E.P., Krishnamoorti, R., Manias, E., 1999. Polymer-silicate nanocomposites: model systems for confined polymers and polymer brushes. Adv. Polym. Sci. 138, 107–147.

Gilman, J.W., 1999. Flammability and thermal stability studies of polymer layered-silicate (clay) nanocomposites. Appl. Clay Sci. 15, 31–49.

Gilman, J.W., Kashiwagi, T., Lichtenhan, J.D., 1997. Nanocomposites: a revolutionary new flame retardant approach. Sample J. 33, 40–46.

Gilman, J.W., Jackson, C.L., Morgan, A.B., Harris, J.R., Manias, E., Giannelis, E.P., Wuthenow, M., Hilton, D., Phillips, S.H., 2000. Flammability properties of polymer – layered-silicate nanocomposites. Polypropylene and polystyrene nanocomposites. Chem. Mater. 12, 1866–1873.

Heeger, A.J., 2002. Semiconducting and metallic polymers: the fourth generation of polymeric materials. Synth. Met. 125, 23–42.

Helfferich, F., Plesset, M.S., 1958. Ion exchange kinetics. A nonlinear diffusion problem. J. Chem. Phys. 28, 418–424.

Instruction Manual, 2000. Scientific Equipment and Services, Roorkee, India.

Khan, A.A., Alam, M.M., 2003. Synthesis, characterization and analytical applications of a new and novel 'organic–inorganic' composite material as a cation exchanger and Cd(II) ion-selective membrane electrode: polyaniline Sn(IV) tungstoarsenate. React. Funct. Polym. 55, 277–290.

Khan, A.A., Khan, A., Inamuddin, 2007. Preparation and characterization of a new organic–inorganic nano-composite poly-*o*-toluidine Th(IV) phosphate: its analytical applications as cation-exchanger and in making ion-selective electrode. Talanta 72, 699–710.

Kojima, Y., Usuki, A., Kawasumi, M., Fukushima, Y., Okada, A., Kurauchi, T., Kamigaito, O., 1993. Synthesis of nylon 6-clay hybrid. J. Mater. Res. 8, 1179–1184.

LeBaron, P.C., Wang, Z., Pinnavaia, T.J., 1999. Polymer-layered silicate nanocomposites: an overview. Appl. Clay Sci. 15, 11–29.

MacDiarmid, A.G., 2002. A novel role for organic polymers. Synth. Met. 125, 11–22.

Messersmith, P.B., Giannelis, E.P., 1995. Synthesis and barrier properties of poly(epsilon-caprolactone)-layered silicate nanocomposites. J. Polym. Sci., Part A: Polym. Chem. 33, 1047–1057.

Mohammad, F., 2000. In: Nalwa, H.S. (Ed.), Handbook of Advanced Electronic and Photonic Materials and Devices. Academic Press, New York, p. 321.

Niwas, R., Khan, A.A., Varshney, K.G., 1998. Preparation and properties of styrene supported zirconium(IV) tungstophosphate: a

mercury(II) selective inorganic–organic ion exchanger. Indian J. Chem. 37, 469–472.
Niwas, R., Khan, A.A., Varshney, K.G., 1999. Synthesis and ion exchange behaviour of polyaniline Sn(IV) arsenophosphate: a polymeric inorganic ion exchanger. Colloids Surf., A 150, 7–14.
Okada, A., Kawasumi, M., Usuki, A., Kojima, Y., Kurauchi, T., Kamigaito, O., 1990. Synthesis and properties of nylon-6/clay hybrids. In: Schaefer, D.W., Mark, J.E. (Eds.), Polymer Based Molecular Composites, MRS Symposium Proceedings, Pittsburgh, USA, vol. 171, pp. 45–50.
Plesset, M.S., Helfferich, F., Franklin, J.N., 1958. Ion exchange kinetics. A nonlinear diffusion problem. II. Particle diffusion controlled exchange of univalent and bivalent ions. J. Chem. Phys. 29, 1064–1069.
Roncoli, J., 1992. Conjugated poly(thiophenes): synthesis, functionalization, and applications. Chem. Rev. 92, 711–738.
Ruoff, R.S., Lorents, D.C., Chan, B., Malhotra, R., Subramoney, S., 1993. Single-crystal metals encapsulated in carbon nanoparticles. Science 259, 346–348.
Saito, Y., Yoshikawa, T., Okuda, M., Ohkohchi, M., Ando, Y., Kasuya, A., Nishina, Y., 1993. Synthesis and electron-beam incision of carbon nanocapsules encaging yc2. Chem. Phys. Lett. 209, 72–76.
Seraphin, S., Zhou, D., Jaio, J., Withers, J.C., Loufty, R., 1993. Yttrium carbide in nanotubes. Nature 362, pp. 503–503.
Shirakawa, H., 2002. The discovery of polyacetylene film: the dawning of an era of conducting polymers. Synth. Met. 125, 3–10.
Tomita, M., Saito, Y., Hayashi, T., 1993. Lac2 encapsulated in graphite nano-particle. Jpn. J. Appl. Phys. 32, L280–L282.
Toshima, N., Hara, S., 1995. Direct synthesis of conducting polymers from simple monomers. Prog. Polym. Sci. 20, 155–183.
Treay, M.M.J., Ebbesen, T.W., Gibson, J.M., 1996. Exceptionally high Young's modulus observed for individual carbon nanotubes. Nature 381, 678–680.
Udum, Y.A., Pekmez, K., Yildiz, A., 2005. Electrochemical preparation of a soluble conducting aniline-thiophene copolymer. Eur. Polym J. 41, 1136–1142.
Vaia, R.A., Price, G., Ruth, P.N., Nguyen, H.T., Lichtenhan, J., 1999. Polymer/layered silicate nanocomposites as high performance ablative materials. Appl. Clay Sci. 15, 67–92.
Varshney, K.G., Gupta, U., Maheshwari, S.M., 1997. Kinetics of ion-exchange of alkaline earth metals on antimony(V) phosphate cation exchanger. React. Kinet. Catal. Lett. 61, 127–132.
Varshney, K.G., Tayal, N., Gupta, U., 1998. Acrylonitrile based cerium (IV) phosphate as a new mercury selective fibrous ion-exchanger – synthesis, characterization and analytical applications. Colloids Surf., A 145, 71–81.
Varshney, K.G., Tyal, N., Khan, A.A., Niwas, R., 2001. Synthesis, characterization and analytical applications of lead (II) selective polyacrylonitrile thorium (IV) phosphate: a novel fibrous ion exchanger. Colloids Surf., A 181, 23–129.
Wang, J.X., 1996. Mechanism of mediation of the electrochemical oxidation of K4Fe(CN)(6) at poly-[tris(3-{omega-[4-(2,2′-bipyridyl)]alkyl}-thiophene)iron(II)]-film modified electrodes in aqueous solutions. Electrochim. Acta 41, 2563–2569.
Wang, Y.D., Rubner, M.F., 1990. Stability studies of the electrical-conductivity of various poly(3-alkylthiophenes). Synth. Met. 39, 153–175.
Wang, C., Guo, Z.X., Fu, S., Wu, W., Zhu, D., 2004. Polymers containing fullerene or carbon nanotube structures. Prog. Polym. Sci. 29, 1079–1141.
Xu, R.U., Manias, E., Snyder, A.J., Runt, J., 2001. New biomedical poly(urethane urea) – layered silicate nanocomposites. Macromolecules 34, 337–339.
Zhang, B., Poojary, D.M., Clearfield, A., Peng, G., 1996. Synthesis, characterization, and amine intercalation behavior of zirconium *N*-(phosphonomethyl)iminodiacetic acid layered compounds. Chem. Mater. 8, 1333–1340.
Zuo, F., Angelopoulos, M., MacDiarmid, A.G., Epstein, A.G., 1987. Transport studies of protonated emeraldine polymer – a antigranulocytes polymeric metal system. Phys. Rev. B 36, 3475–3478.